Original Article

Fe₃O₄@SiO₂@Mel-Rh-Cu: A High-Performance, Green Catalyst for Efficient Xanthene Synthesis and Its Application for Magnetic Solid Phase Extraction of Diazinon Followed by Its Determination through HPLC-UV

Sahar Peiman[1] , Behrooz Maleki[1],* , Milad Ghani[2]

[1]*Department of Organic Chemistry, Faculty of Chemistry, University of Mazandaran, Babolsar, Iran*
[2]*Department of Analytical Chemistry, Faculty of Chemistry, University of Mazandaran, Babolsar, Iran*

A R T I C L E I N F O

A B S T R A C T

A novel, high-performance, recyclable heterogeneous catalyst functionalized with melamine was advantageously prepared and rhodanine on magnetic silica was successfully carried out. After that, the Cu ions were coordinated with the existing ligands decorated on the magnetic silica surface. This catalyst was identified by different analyses and acted as a recoverable catalyst for xanthene synthesis. Its advantages include the solvent-free conditions of the reaction, the high efficiency of the products in a short period of time, as well as its simple collection from the reaction environment. Moreover, the prepared sorbent has been developed for the extraction of diazinon from different real samples through magnetic solid phase extraction (MSPE). Under optimal conditions, the linear range for measuring diazinon was 0.5-200 μg L^{-1}. The coefficient of determination (R^2) was 0.9985. The limit of detection (LOD) of the method was 0.08 μg L^{-1}. Relative standard deviation values (RSD%) for the concentration of 10.0 μg L^{-1} and 100 μg L^{-1} were between 5.3% and 5.9%. Finally, the proposed method was used to determine diazinon in orange and agricultural water. The results showed that the percentage of relative recovery of the selected toxin in the studied real samples was between 92 and 105.

G R A P H I C A L A B S T R A C T
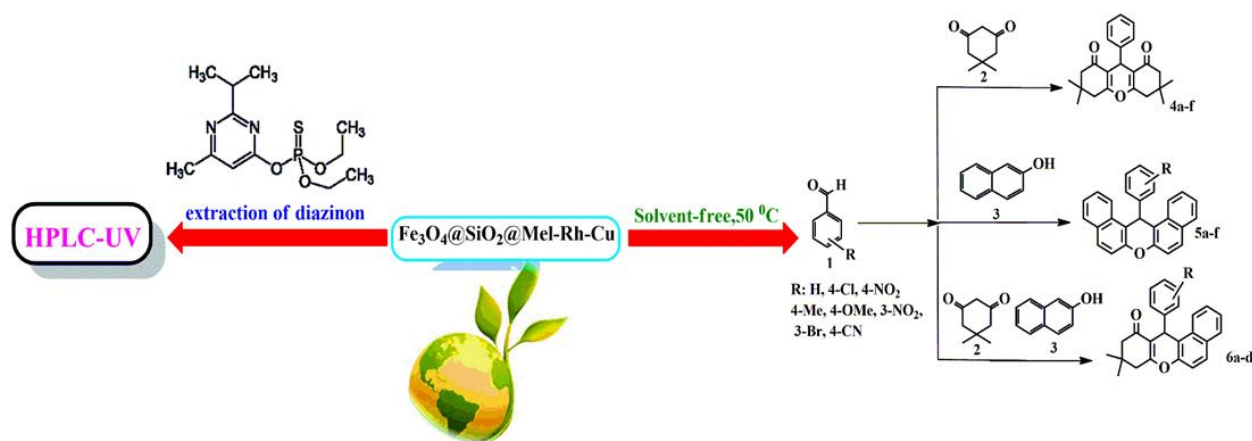
Introduction

Heterocyclic compounds are a clear example of chemical structures that have important roles and functions in human life. In addition to carbon, this category of organic compounds has heteroatoms instance as nitrogen, oxygen, or sulfur. Heterocyclic compounds have wide and vital applications in various industries and biological fields. Among its applications in industries, we can mention the production of paints, antioxidants, antimicrobial herbicides, corrosion inhibitors, copolymers, and agriculture. They are also mainly in the structure of many drugs such as penicillin, and cephalosporin; There are alkaloids like vinblastine, morphine, reserpine, *etc.* [1-4].

Xanthene and benzoxanthene are an important group of three-ring heterocycles containing oxygen and are biologically active. They are an important group of compounds with different uses for example anti-tumor, anti-viral, anti-inflammatory activities, food additives, and anti-fungal [5-9].

In the past years, the study of rhodanine and its derivatives, which are a main group of heterocyclic structures, has been of particular importance. Rhodanines are present in the chemical skeleton of drugs like the behavior toward type II diabetes, Alzheimer's disease, cancer, and cataracts. These compounds have antibacterial, antifungal, antiviral, antimalarial, insecticide and herbicide activities [10-13].

In recent decades, the use of nanomaterials, especially magnetic nanoparticles, has become very popular in various fields such as drug delivery. Magnetic nanoparticles are of interest owing to their unique characteristics like easy separation, high recyclability, large surface area, proper dispersion, and low toxicity [14-19].

Many coating materials such as noble metals, polymers, and silica have been used for magnetic nanoparticles. Among the various coatings of biocompatible and hydrophilic silica material due to the preservation of nanoparticles against various environmental factors for example changes in pH and air, as well as the presence of silanol groups on its surface, which easily connects with molecules and ligands, is more important, and can be used in biomedical fields [20,21].

Copper (Cu) nanoparticles are cheap, have good efficiency, low catalyst loading, and short reaction time among their advantages. They are used in various fields such as water purification, heat transfer systems, and biomedicine, and also have antibacterial activity. To overcome the problems that limit the activity of catalysts such as aggregation, oxidation, and difficult separation, they are placed on various substrates like silica, organometallic frameworks, polymers, and zeolites [21,22].

In this way, in continuation of the past catalytic works [23,29] and to develop a new practical method, we designed a green novel catalyst system on a magnetic silica substrate based on melamine and rhodanine. Then, this

heterogeneous catalyst (Fe$_3$O$_4$@SiO$_2$@Mel-Rh-Cu) was used in the synthesis reaction of xanthenes, which are heterocyclic compounds. In the next part of this study, the prepared sorbent was used for the MSPE of diazinon The Box-Behnken Design (BBD) and Response Surface Methodology (RSM) were used to optimize the practical extraction factors after they had been tested with the Plackett-Burman Design (PBD). Pesticides are widely used in the cultivation of plants and plant products to prevent and control diseases and insect pests. Pesticides include insecticides, fungicides, herbicides, or a combination of one or more types of chemicals that are used primarily in agriculture to kill pests. Toxin concentrations in plants and agricultural products should be measured. Due to the presence of pesticides and their high toxicity, it is nowadays important to develop and extend methods to determine the amount of pesticide residues in fruit and water samples. The toxic effects of diazinon are due to inhibition of acetylcholinesterase. Diazinon is an insecticide, and one of its detection methods is chromatography, which offers a low level of detection but requires the pretreatment of samples before analysis. Therefore, it is important to provide an affordable and reliable method to measure toxins.

Here, the magnetic sorbent was used for the presentation of a novel extraction method. The obtained results showed good extraction efficiency, no memory effect, high adsorption capacity, and good reproducibility. Therefore, the desired adsorbent can be used to extract different analytes in real samples.

Experimental

Each of the solvents or materials is from Merck and Fulica. NMR (^{1}H and ^{13}C) spectra were measured with a Bruker DRX-400 AVANCE spectrometer. Melting points were calculated using the Electrothermal IA9100 (Essex, UK). XRD was performed using the PHILIPS, PW1730 instrument. TGA was performed with a Netzsch device (Selb, Germany). The SEM and VSM analyses were performed using TESCAN MIRA III

and MDKB Kashan Desert Magnet Company. The power of the external magnet is 1.2 T.

Synthesis of Fe$_3$O$_4$@SiO$_2$

Magnetic nanoparticles were synthesized according to the published literature [21]. In the next step, Stober's method was used to synthesize Fe$_3$O$_4$@SiO$_2$. 1 g Fe$_3$O$_4$ in ethanol (100 mL), and deionized water (50 mL) was sonicated (40 min), and then 25% ammonia was added to the reaction (4 mL). TEOS (Tetraethyl orthosilicate) (4 mL, 3.73 g) was then added dropwise and stirred for 18 h. The Fe$_3$O$_4$@SiO$_2$ was collected by a magnetic field, washed with water/ethanol, and dried.

Synthesis of Fe$_3$O$_4$@SiO$_2$@CPTMS

Initially, 1 g Fe$_3$O$_4$@SiO$_2$ was dispersed in dry toluene for 35 min. 1 mL (1.09 g) 3-chloropropyltrimethoxysilane (CPTMS) was added under reflux conditions and N$_2$ atmosphere. After 18 h, the reaction mixture was filtered and washed with toluene [30].

Synthesis of Fe$_3$O$_4$@SiO$_2$@Mel

1 g of Fe$_3$O$_4$@SiO$_2$@CPTMS was dispersed in 50 ml of ethanol. Then 2 mmol of melamine was added and refluxed for 22 h. The prepared Fe$_3$O$_4$@SiO$_2$@Melamine (Fe$_3$O$_4$@SiO$_2$@Mel) was washed with ethanol/water and dried [31].

Synthesis of Fe$_3$O$_4$@SiO$_2$@Mel-Rh

Initially, 1 g of Fe$_3$O$_4$@SiO$_2$@Mel in 30 ml of dry toluene was placed under ultrasonic radiation for 30 min to disperse it well. Then 3 ml (3.48 g) of 1, 4-dichlorobutane and 2 mmol (0.33 g) of KI were added to the solution, it was kept for 18 h under reflux and nitrogen conditions. The resulting mixture was separated from the solvent with the help of a magnet, washed multiple times with ethyl acetate, and dried at 60 °C [30]. In the next step, 1 g of synthetic material from the former stage was dispersed in DMF for 30 min. 3 mmol (0.4 g) of rhodanine, was added and stirred at 90 °C for 30 h. Fe$_3$O$_4$@SiO$_2$@Melamine-rhodanine

(Fe₃O₄@SiO₂@Mel-Rh) was washed with water after separation [30].

Synthesis of Fe₃O₄@SiO₂@Mel-Rh-Cu

1 g of Fe₃O₄@SiO₂@Mel-Rh was dispersed in water by ultrasonic waves, and then 0.1 g Cu(OAc)₂ was added and stirred for 15 h at 80 °C. The resulting was separated by a magnetic field and washed with deionized water (Scheme 1).
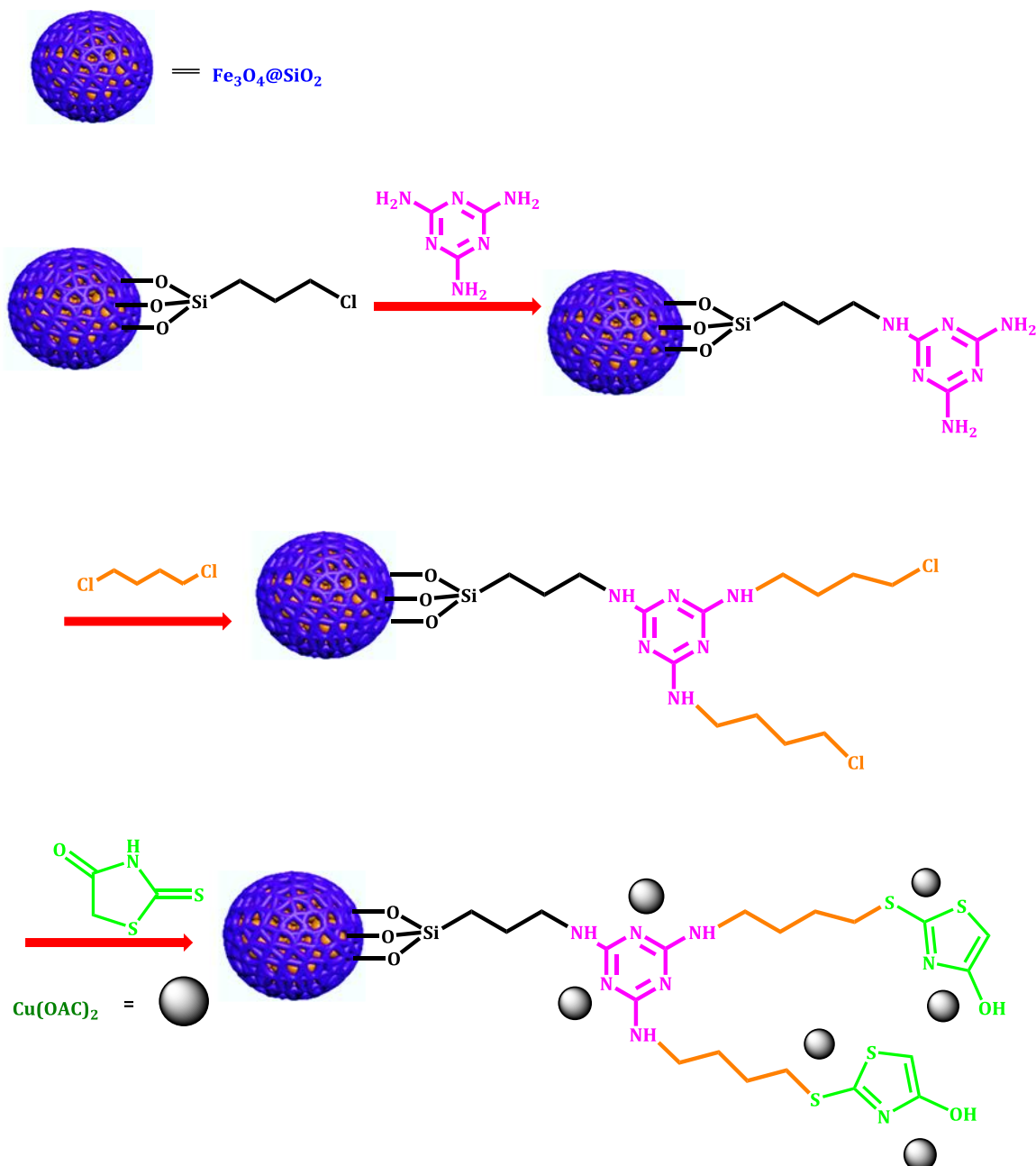
Scheme 1: Catalyst synthesis steps Fe₃O₄@SiO₂@Mel-Rh-Cu

General Procedure for the Synthesis of Xanthenes

The arylaldehyde (1 mmol), dimedone (1 mmol, 0.14 g), and 2-naphthol (1 mmol, 0.14 g) were mixed together in the presence of

Fe₃O₄@SiO₂@Mel-Rh-Cu catalyst under solvent-free conditions at 50 °C. Finally, ethanol was added to the reaction mixture and the Fe₃O₄@SiO₂@Mel-Rh-Cu was separated using a

magnetic field. The resulting precipitate was recrystallized in ethanol (Scheme 2).
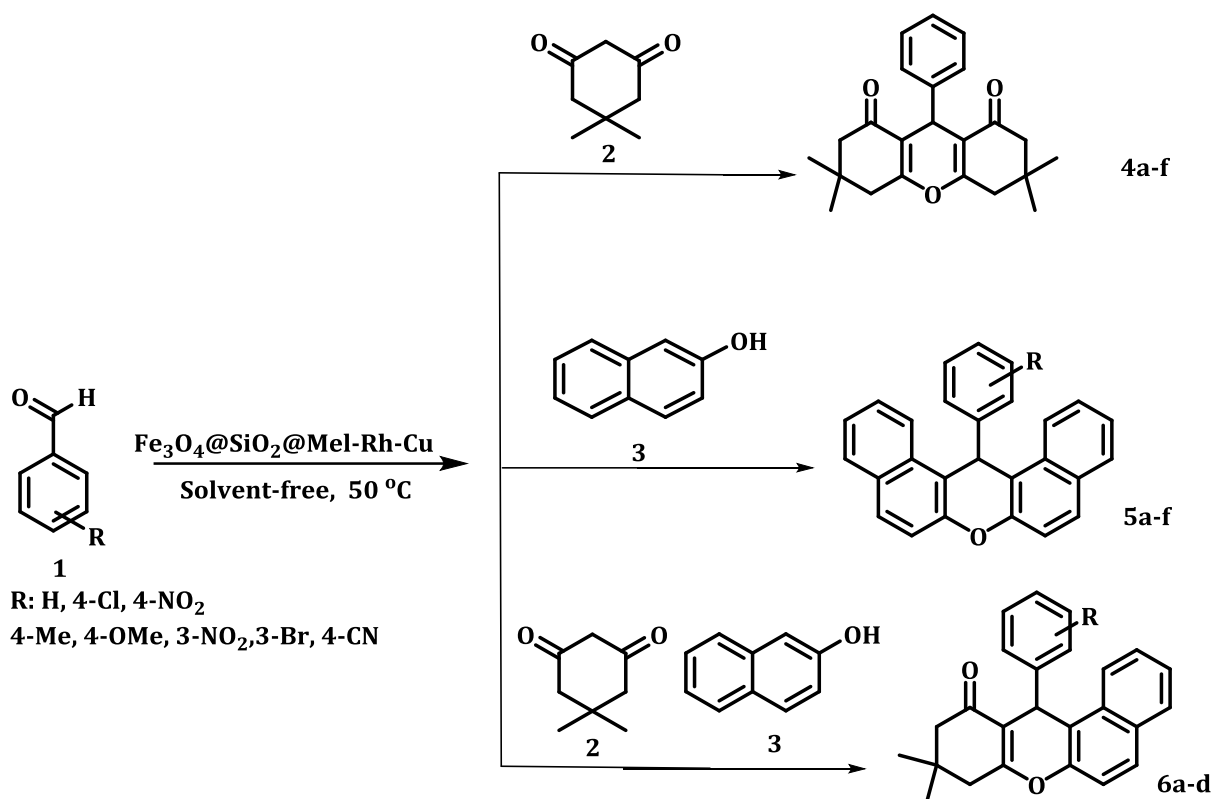
Scheme 2: Synthesis of xanthenes using Fe₃O₄@SiO₂@Mel-Rh-Cu

Selected Spectral Data

3,3,6,6-Tetramethyl-9-phenyl-3,4,5,6,7,9-hexahydro-1H-xanthene-1,8(2H)-dione (4a):

^{1}H-NMR (CDCl₃, 400 MHz): δ 1.03 (s, 6H), 1.14 (s, 6H), 2.20 and 2.26 (4H, J=16.0 Hz,), 2.50 (s, 4H), 4.75 (s, 1H), and 7.20–7.27 (m, 4H). ^{13}C-NMR (CDCl₃, 100 MHz): δ 26.4, 30.0, 31.5, 33.4, 39.9, 49.5, 114.6, 129.0, 130.0, 133.1, 143.4, 163.5, and 197.1.

9-(4-Methoxyphenyl)-3,3,6,6-tetramethyl-3,4,5,6,7,9-hexahydro-1H-xanthene-1,8(2H)-dione (4d):

^{1} H-NMR (CDCl₃, 400 MHz): δ 1.00 (s, 6H), 1.15 (s, 6H), 2.17 and 2.30 (4H, CH₂), 2.51 (s, 4H), 4.85 (s, 1H), 7.50 (d, 2H), and 8.15 (d, 2H). ^{13}C NMR (CDCl₃, 100 MHz): δ 26.9, 30.0, 31.3, 33.6, 41.0, 51.0, 111.0, 115.1, 123.5, 130.1, 147.4, 151.5, 163.0, and 196.2.

14-Phenyl-14H-dibenzo[a,j]xanthene (5a):

δ ^{1}H-NMR (CDCl₃, 400 MHz): δ 6.50 (s, 1H), 7.13 (d, 2H), 7.43–7.52 (m, 6H), 7.60–7.64 (m, 2H), 7.83 (d, 2H), 8.56 (d, 2H), and 8.34 (d, 2H). ^{13}C-NMR (CDCl₃, 100 MHz): δ 38.4, 117.8, 119.2, 121.5, 125.4, 127.9, 128.8, 129.0, 129.1, 129.5, 131.1, 131.3, 132.1, 143.5, and 148.7.

9-Dimethyl-12-(4-nitrophenyl) -9,10-dihydro-8H-benzo[a]xanthen-11(12H) -one (6c):

^{1}H-NMR (CDCl₃, 400 MHz): δ 0.97 (s, 3H, CH₃), 1.16 (s, 3H, CH₃), 2.25 and 2.38 (2H, , CH₂), 2.62 (s, 2H, CH₂), 5.84 (s, 1H, CH), 7.38 (d, 1H, CH), 7.40-7.48 (m, 2H, CH), 7.54 (d, 2H, CH), 7.81-7.86 (m, 3H, CH), and 8.05 (d, 2H, CH). ^{13}C-NMR (CDCl₃, 100 MHz): δ 27.0, 29.3, 32.2, 34.9, 41.4, 50.7, 112.9, 116.0, 117.1, 123.1, 123.6, 125.2, 127.3, 128.6, 129.3, 129.6, 131.0, 131.5, 146.3, 151.8, 164.6, and 196.7.

12-(3-Bromophenyl)-9,9-dimethyl-9,10-dihydro-8H-benzo[a]xanthen-11(12H)-one (6d):

^{1}H-NMR (CDCl$_3$, 400 MHz): δ 0.98 (s, 3H), 1.17 (s, 3H), 2.25 and 2.38 (2H, CH$_2$), 2.73 (s, 2H), 5.78 (s, 1H), 7.39 (d, 1H), 7.41-7.50 (m, 2H), 7.59 (d, 2H), 7.83-7.88 (m, 3H), 8.08 (d, 2H). ^{13}C-NMR (CDCl$_3$, 100 MHz): δ 26.9, 30.0, 33.2, 35.0, 41.45, 51.0, 113.0, 116.1, 117.2, 123.2, 123.8, 125.6, 127.5, 128.9, 129.8, 129.3, 131.1, 131.3, 146.7, 151.9, 164.2, and 196.8.

Results and Discussion

We report in this research the synthesis and characterization of a novel heterogeneous catalyst of Cu(OAc)$_2$ immobilized on a magnetic silica substrate. For this purpose, magnetic silica was first prepared using literature, and then 3-chloropropyltrimethoxysilane was used to connect the substrate with melamine. The next step involves the grafting of melamine to rhodanine *via* a 1,4-dichlorobutane as the linker. Subsequently, in the final step, copper (II) acetate was utilized for the metal coordination complex to provide Fe$_3$O$_4$@SiO$_2$@Mel-Rh-Cu.

Characterization of Catalyst

After the synthesis of the catalyst, FT-IR TGA, XRD, FESEM, EDX, elemental mapping, VSM, and ICP techniques were used to identify it.

In the FT-IR spectrum, the peak in the regions of 590, 956, and 1063 cm^{-1} is associated with the stretching vibrations of Fe-O, Si-O-Fe, and Si-O bonds, respectively. C-H stretching vibrations appear in the range of 2922-2983 cm^{-1}. The peak in the range of 1230 cm^{-1} refers to CH$_2$-Cl bending (in the spectrum of Fe$_3$O$_4$@SiO$_2$@CPTMS). The presence of peaks in the 1548 and 1650 cm^{-1} regions is attributed to the stretching vibrations of C=C, C=N, and the characteristic peaks at 3338-3469 cm^{-1} are also associated with NH and NH$_2$ groups, which indicates the successful connection of the melamine ring to the substrate (in the spectrums of melamine, and Fe$_3$O$_4$@SiO$_2$@Mel@Cl (Figure 1).
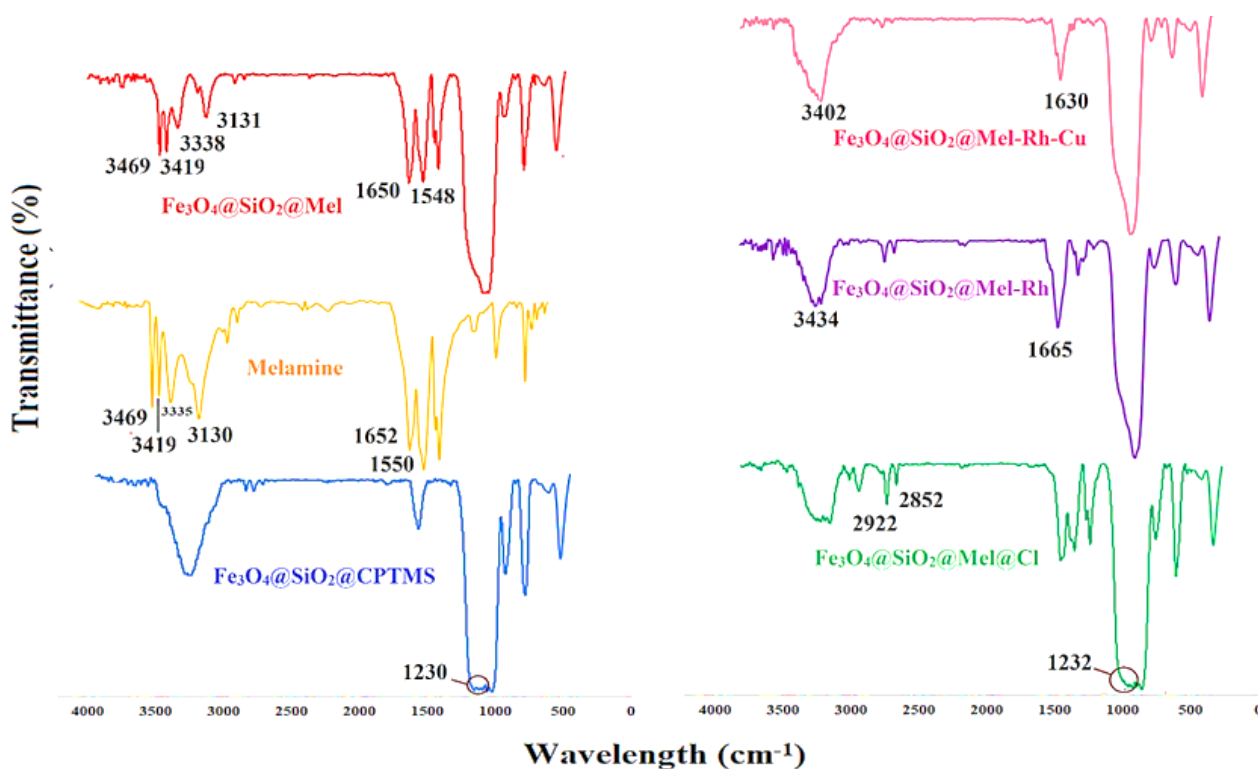

Figure 1: FTIR spectrum of Fe$_3$O$_4$@SiO$_2$@Mel-Rh-Cu synthesis steps

The increase in the height of the peak in the region of 2852-2922 cm^{-1} and the peak in the region 1232 cm^{-1} corresponding to C–H wag (–CH$_2$-Cl) stretching presence of alkyl halides (in the spectrum of Fe$_3$O$_4$@SiO$_2$@Mel@Cl) indicates the binding of 1,4-dichlorobutane to melamine. C-N stretching bond of rhodanine appeared at 1665 cm^{-1} and OH stretching vibrations were also attributed to 3434 cm^{-1} (in the spectrum of Fe$_3$O$_4$@SiO$_2$@Mel-Rh-Cu), which proof of rhodanine is binding. FT-IR spectrum was analyzed to confirm the metallization of Fe$_3$O$_4$@SiO$_2$@Mel-Rh. The change in curves Fe$_3$O$_4$@SiO$_2$@Mel-Rh-Cu from 1665 to 1630 cm^{-1} and 3433 to 3402 cm^{-1} associated with C-N and OH stretching bond is attributed to coordination with metal.

TGA curve is used to determine the percentage of supported organic functional groups on the Fe$_3$O$_4$@SiO$_2$@Mel-Rh-Cu catalyst surface in Figure 2. Weight loss at temperatures below 200 °C is related to the removal of surface water. 20 % weight loss at 300 to 800 °C is associated with the decomposition of organic groups placed on the Fe$_3$O$_4$@SiO$_2$ substrate (Figure 2).
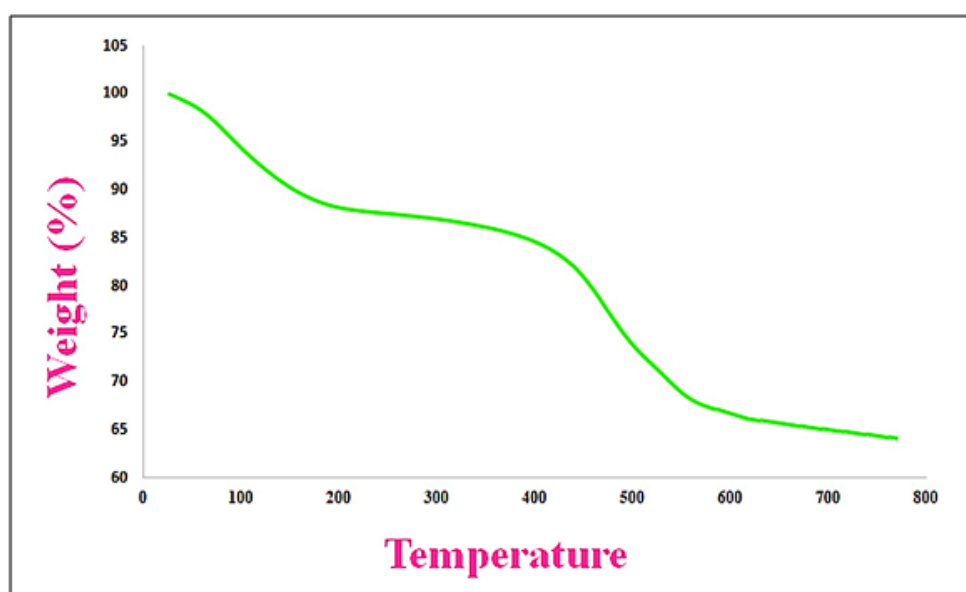
Figure 2: TGA curve of Fe$_3$O$_4$@SiO$_2$@Mel-Rh-Cu

Through XRD analysis of Fe$_3$O$_4$, Fe$_3$O$_4$@SiO$_2$@Mel-Rh, and Fe$_3$O$_4$@SiO$_2$@Mel-Rh-Cu, their crystal structure was investigated. The XRD patterns of all three compounds show six diffraction peaks related to the inverse cubic spinel structure of Fe$_3$O$_4$ at 2θ : 30.26° (220), 35.86° (311), 43.25° (400), 53.22° (422), and 57.01° (511) which indicates the preservation of the crystal structure of the composition after modification. Due to the dispersion of Cu nanoparticles in the matrix, which cannot form a regular crystal lattice, no diffraction peak for Cu nanoparticles was observed for Fe$_3$O$_4$@SiO$_2$@Mel-Rh-Cu.The immobilization of Cu species was confirmed by IR, ICP-OES and EDX analysis (Figure 3).

The morphology of the synthesized nanocatalyst was considered by SEM analysis. FE-SEM images of Fe$_3$O$_4$ show the spherical shape of nanoparticles with a size of 8 nm. After placing the silica layer, the organic ligands of the catalyst morphology were preserved and the diameter of the Fe$_3$O$_4$@SiO$_2$@Mel-Rh-Cu nanoparticles increased to an average of 23 nm (Figure 4).
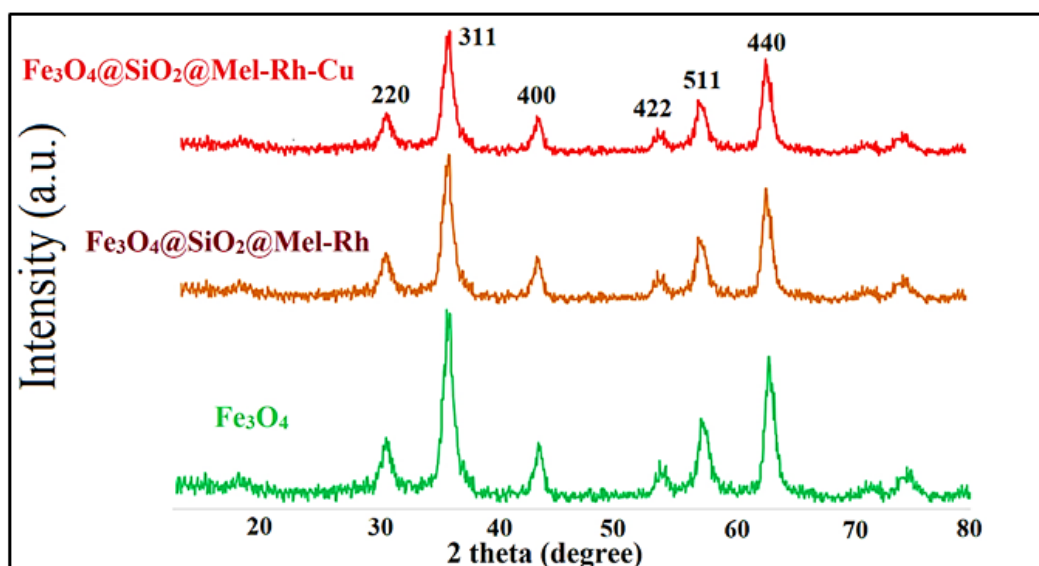
Figure 3: XRD patterns of Fe_3O_4, $Fe_3O_4@SiO_2@Mel-Rh$ and, $Fe_3O_4@SiO_2@Mel-Rh-Cu$
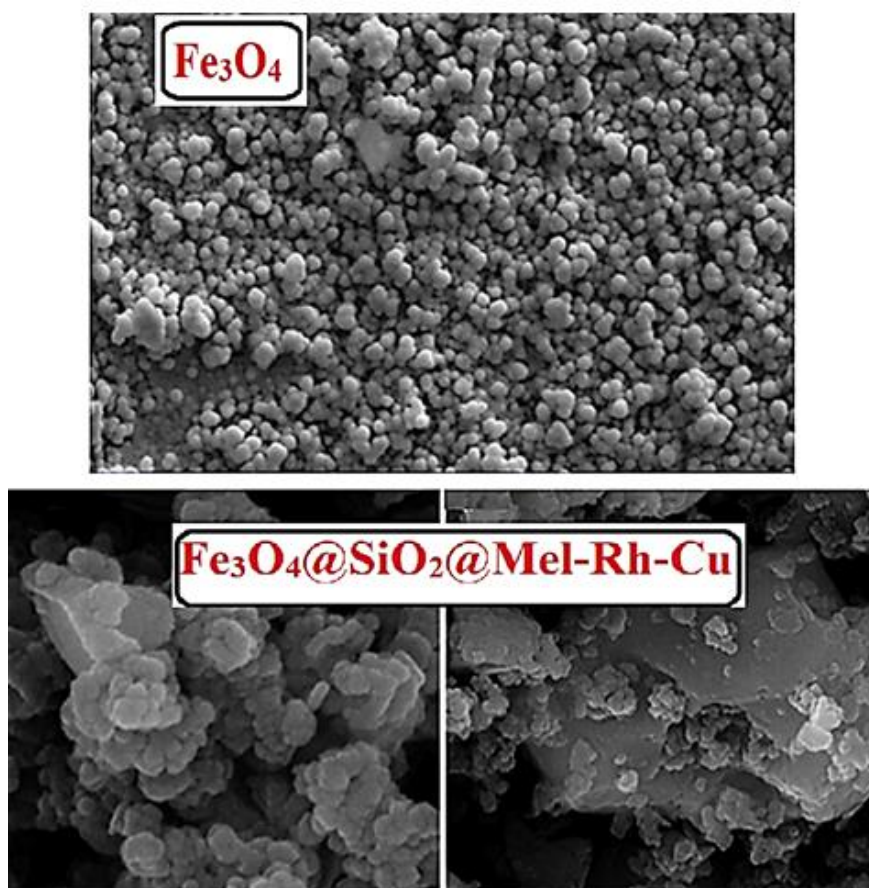
**Figure 4:** SEM analysis of Fe_3O_4 and $Fe_3O_4@SiO_2@Mel-Rh-Cu$

The EDX analysis confirmed the elements Fe, Si, O, C, S, and N (Figure 5). The analysis of the element distribution also shows a uniform distribution of these elements on the surface of the $Fe_3O_4@SiO_2@Mel-Rh-Cu$ (Figure 6).
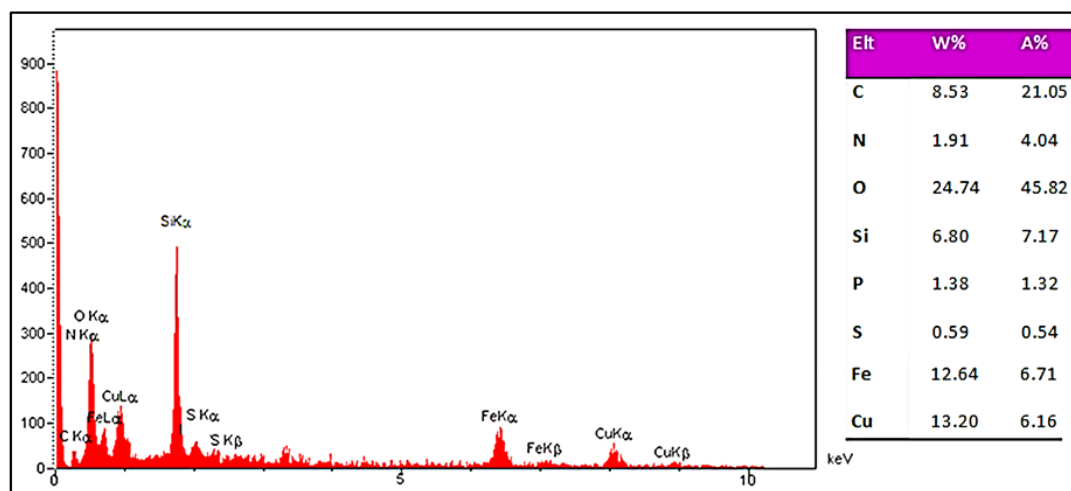
**Figure 5:** EDx pattern of Fe$_3$O$_4$@SiO$_2$@Mel-Rh-Cu
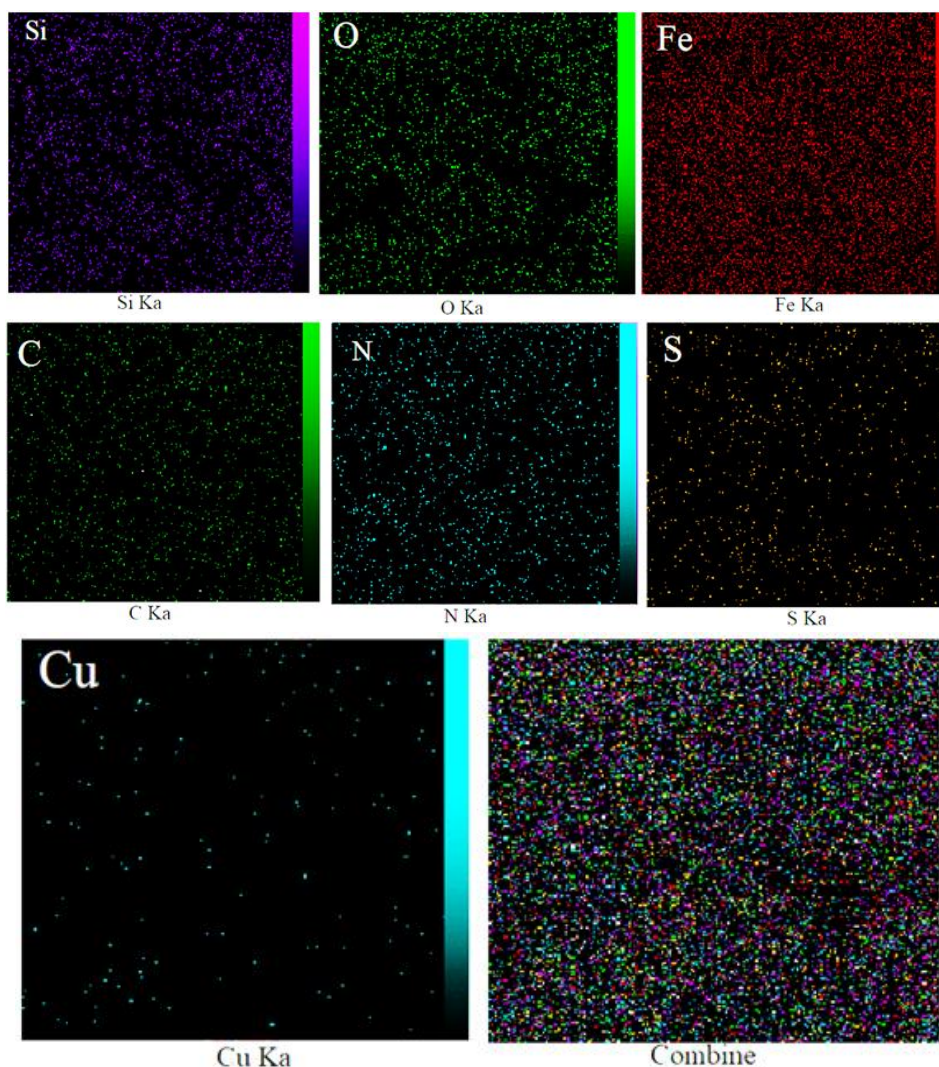
Figure 6: Elemental mapping of Fe$_3$O$_4$@SiO$_2$@Mel-Rh-Cu

Analysis of the magnetic properties of Fe$_3$O$_4$ and Fe$_3$O$_4$@SiO$_2$@Mel-Rh-Cu was done by VSM analysis. The magnetic curve for Fe$_3$O$_4$ and Fe$_3$O$_4$@SiO$_2$@Mel-Rh-Cu showed 65 and 47 emu/g, respectively. The saturation magnetization of the Fe$_3$O$_4$@SiO$_2$@Mel-Rh-Cu

has decreased due to the silica coating and the diamagnetic contribution of the added organic parts. However, the magnetic property of the

catalyst is still well preserved and it is easily separated from the solution (Figure 7).
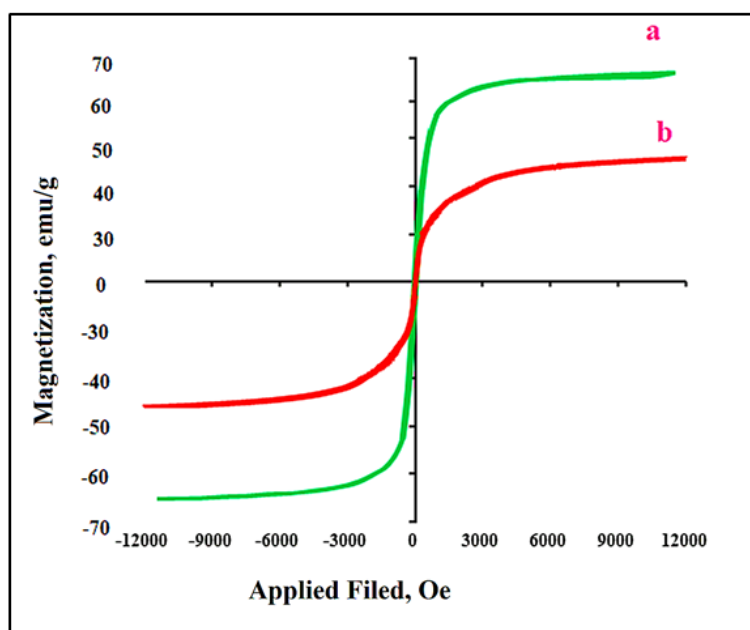
Figure 7: Magnetization curves of (a) Fe_3O_4 and (b) $Fe_3O_4@SiO_2@Mel-Rh-Cu$

Finally, based on ICP analysis, the exact loading of Cu on the surface of the synthesized catalyst was found to be 2.96 mmol/g.

To illustrate the power and efficiency of the synthesized catalyst, we measured its activity in the synthetic reaction between aromatic aldehydes, dimedone, or 2-naphthol. For this purpose, the reaction between 4-chlorobenzaldehyde (1 mmol, 0.14 g) and dimedone (2 mmol, 0.14 g) was selected as the model until the optimal conditions were reached. Initially, the reaction was accomplished in solvents for instance ethanol, methanol, dichloromethane, acetonitrile, dimethylformamide, and solvent-free conditions. It was observed that solvent-free conditions are the most suitable choice for this catalyst in the reaction (Table 1, entries 1-6). The reaction efficiency was also evaluated in temperature conditions (25 to 80 °C). The observations indicated that increasing the temperature by more than 50 °C did not influence the reaction

yield (Table 1, entries 6-9). The best amount of catalyst (estimated between 10-40 mg) was calculated as 20 mg (Table 1, entries 6 and 10-13). Finally, without a catalyst, the reaction was performed, which showed a trace yield of the product (Table 1, entry 14).

Investigating and Optimizing the Type of Desorption Solvent

The choice of the type of solvent and adsorption is a very effective parameter for the extraction process. A suitable solvent can desorb the adsorbed analytes with the smallest volume from the surface of the adsorbent. In this study, the solvents acetonitrile, methanol, ethanol, isopropanol and ethyl acetate were selected for the desorption process. The results showed that methanol exhibited better efficiency than the other solvents used. Therefore, methanol was chosen as the most suitable desorption solvent (Figure 8).
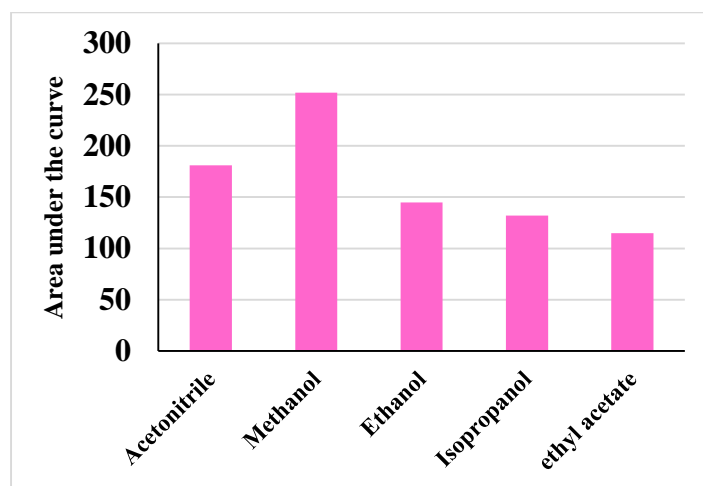
Figure 8: The effect of type of desorption solvent on magnetic solid phase microextraction process

After determining the optimal conditions, to expand the reaction range, different aromatic aldehydes with dimedone (**2**) and/or 2-naphthol (**3**) were used in the presence of Fe_3O_4@SiO_2@Mel-Rh-Cu (Table 2). The outcomes are displayed in the electron-withdrawing groups unlike electron-donating groups will increase the efficiency and decrease the reaction time.

Table 1: Optimization of reaction conditions[a]

Entry	Catalyst (mg)	Solvent	Temperature (°C)	Time (min)	Yield[b] (%)
1	Fe_3O_4@SiO_2@Mel-Rh-Cu (20)	EtOH	50	15	85
2	Fe_3O_4@SiO_2@Mel-Rh-Cu (20)	MeOH	50	15	75
3	Fe_3O_4@SiO_2@Mel-Rh-Cu (20)	CH_2Cl_2	50	15	52
4	Fe_3O_4@SiO_2@Mel-Rh-Cu (20)	CH_3CN	50	15	70
5	Fe_3O_4@SiO_2@Mel-Rh-Cu (20)	DMF	50	15	80
6[b]	**Fe_3O_4@SiO_2@Mel-Rh-Cu (20)**	**Solvent-free**	**50**	**15**	**98**
7	Fe_3O_4@SiO_2@Mel-Rh-Cu (20)	Solvent-free	25	15	82
8	Fe_3O_4@SiO_2@Mel-Rh-Cu (20)	Solvent-free	60	15	98
9	Fe_3O_4@SiO_2@Mel-Rh-Cu (20)	Solvent-free	80	15	98
10	Fe_3O_4@SiO_2@Mel-Rh-Cu (10)	Solvent-free	50	15	60
11	Fe_3O_4@SiO_2@Mel-Rh-Cu (15)	Solvent-free	50	15	80
12	Fe_3O_4@SiO_2@Mel-Rh-Cu (30)	Solvent-free	50	15	98
13	Fe_3O_4@SiO_2@Mel-Rh-Cu (40)	Solvent-free	50	15	98
14	-	Solvent-free	50	15	Trace

[a]*Reaction conditions: 1 mmol 4-chlorobenzaldehyde, 2 mmol dimedone, in the presence of Fe_3O_4@SiO_2@Mel-Rh-Cu*
[b]*Isolated yield. The bold values of entry 6 correspond to the optimal condition*

Table 2: Synthesis xanthenes using Fe₃O₄@SiO₂@Mel-Rh-Cu ᵃ
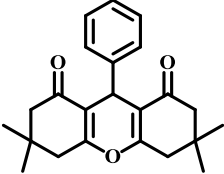
Entry	Product	Time (min)	Yield ᵃ (%)	M.P. °C [Ref.]
1	**4a**	17	96	204–205 [32]
2	**4b**	15	98	233–235 [32]
3	**4c**	15	98	230–232 [32]
4	**4e**	25	90	229–230 [33]
5	**4d**	20	92	252–253 [32]
6	**4e**	25	92	166–168 [32]
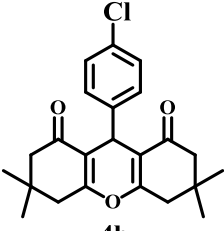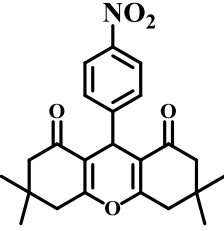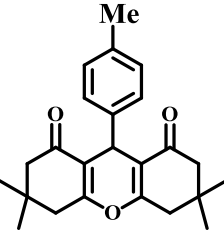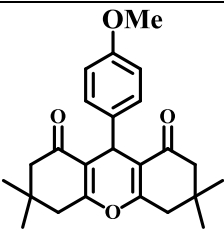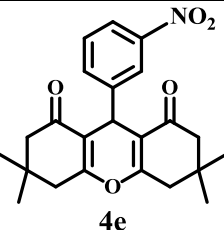
Entry	Product	Time (min)	Yield [a] (%)	M.P. °C [Ref.]
7	4f	20	95	286–287 [32]
8	5a	18	98	284–285 [32]
9	5b	20	95	284–285 [32]
10	5c	17	95	316–318 [32]
11	5d	25	88	220–221 [34]
12	5e	20	85	202–204 [32]
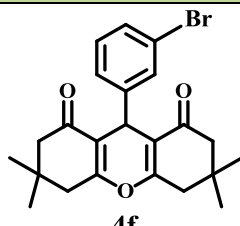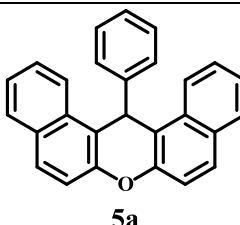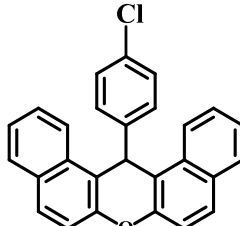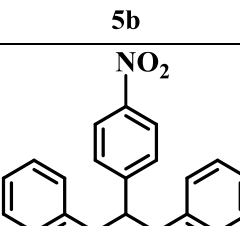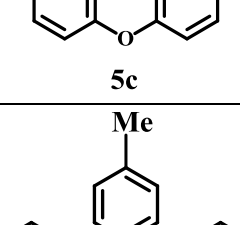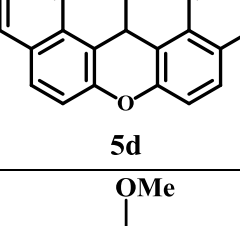
Entry	Product	Time (min)	Yield [a] (%)	M.P. °C [Ref.]
13	5f	20	88	215–216 [32]
14	6a	20	94	176–177 [32]
15	6b	20	96	199–201 [35]
16	6c	20	98	173–174 [32]
17	6d	22	86	160–161 [32]
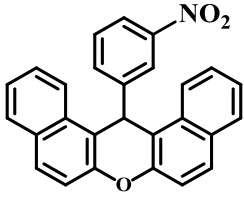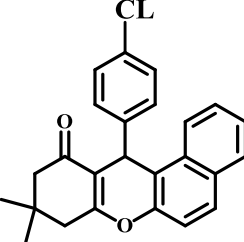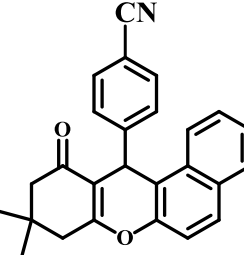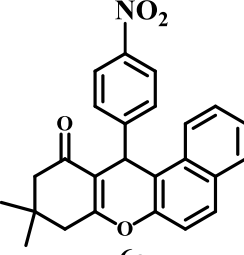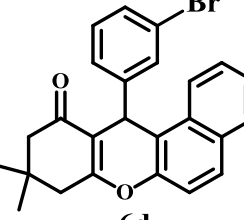
[a]*Reaction conditions: aldehydes (1 mmol), dimedone (2 mmol), or 2-naphthol (2 mmol), and $Fe_3O_4@SiO_2@Mel$-Rh-Cu (20 mg) in solvent-free conditions*

In the next step, the performance of the synthetic catalyst was compared with the previously published results (Table 3). The technique used is simpler, easier to separate, more effective, and with higher yields in less time for this reaction than other methods.

Table 3: Fe$_3$O$_4$@SiO$_2$@Mel-Rh-Cu catalyst comparison with some reported catalysts

Compounds	Conditions	Time	Yield (%)
	present work/solvent-free/50 °C	15 min	98
	Zr (DP)$_2$ / EtOH/reflux [36]	24 h	98
	SBSSA/ EtOH/reflux [37]	10 h	98
	ZnO–CH$_3$COCl/CH$_3$CN/reflux [38]	5 h	90
	boric acid/solvent free/120 °C [39]	20 min	96
	perlite NPs@IL/ZrCl4/solvent free/80 °C [40]	2 h	51
	Fe^{3+}-montmorillonite EtOH/100 °C [41]	30 min	98
	present work/solvent free/50 °C	20 min	98
	CuSO$_4$/SiO$_2$ / Solvent free [42]	75 min	91
	TBAHS / H$_2$O [43]	2.5 h	86
	PWA / Solvent free [44]	50 min	90
	P-TSA / [bmim]BF$_4$ [45]	2.5 h	92
	PEG-400 [46]	6 h	89
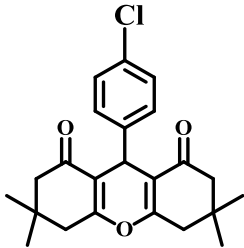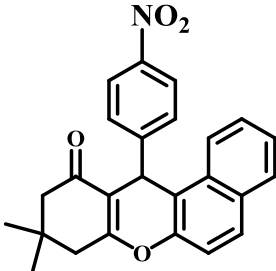
Synthesis Mechanism of Xanthene Derivatives by Fe$_3$O$_4$@SiO$_2$@Mel-Rh-Cu

At the beginning of the reaction, the carbonyl group of aldehydes is activated by the catalyst so that the nucleophilic attack can be carried out more easily. Intermediate A is formed by the attack of dimedone on aldehyde, and then by adding another molecule of dimedone to that intermediate B, and finally by removing the water molecule, the desired product is created (Scheme 3).

One of the important processes in the synthesis of catalysts is their recovery and reusability. To check this, the reaction of the model was used. Subsequent to the ending of the reaction, the Fe$_3$O$_4$@SiO$_2$@Mel-Rh-Cu was collected by the magnetic field and washed with ethanol and after drying, it was used in a further step. This catalyst can be reused for at least 7 steps. Likewise, after seven consecutive cycles of reuse of Fe$_3$O$_4$@SiO$_2$@Mel-Rh-Cu, the XRD patterns, and FT-IR spectra do not indicate remarkable differences with the fresh figure, and the properties and activity of the catalyst remain unchanged (Figure 9).

Preparation of Real Samples

The purpose of this study was to investigate the ability of the prepared adsorbent in to measure the real samples of oranges and agricultural waste water. The desired sample was bought from a local market and after washing with water, it was peeled and crushed completely. To provide the samples, 10 g of it was crushed and added to 15 ml of acetonitrile and 5 ml of water. Further, 1 g of NaCl was added to the solution and the resulting mixture was ultrasonicated (min). Finally, 4 g of MgSO$_4$ was added to the mixture and the mixture was centrifuged for 5 min. Thereafter, 5 mL of the supernatant was removed and centrifuged again for (3 min). The resulting solution was used to extract target analytes. The standard addition method was used for quantifying tasks. For this purpose, standard concentrations of 2, 5, and 10 μg L^{-1} of target analytes were added to the samples. After the extraction process, finally, the extracted eluents were injected into HPLC-UV and the concentration of diazinon in the real samples was determined.
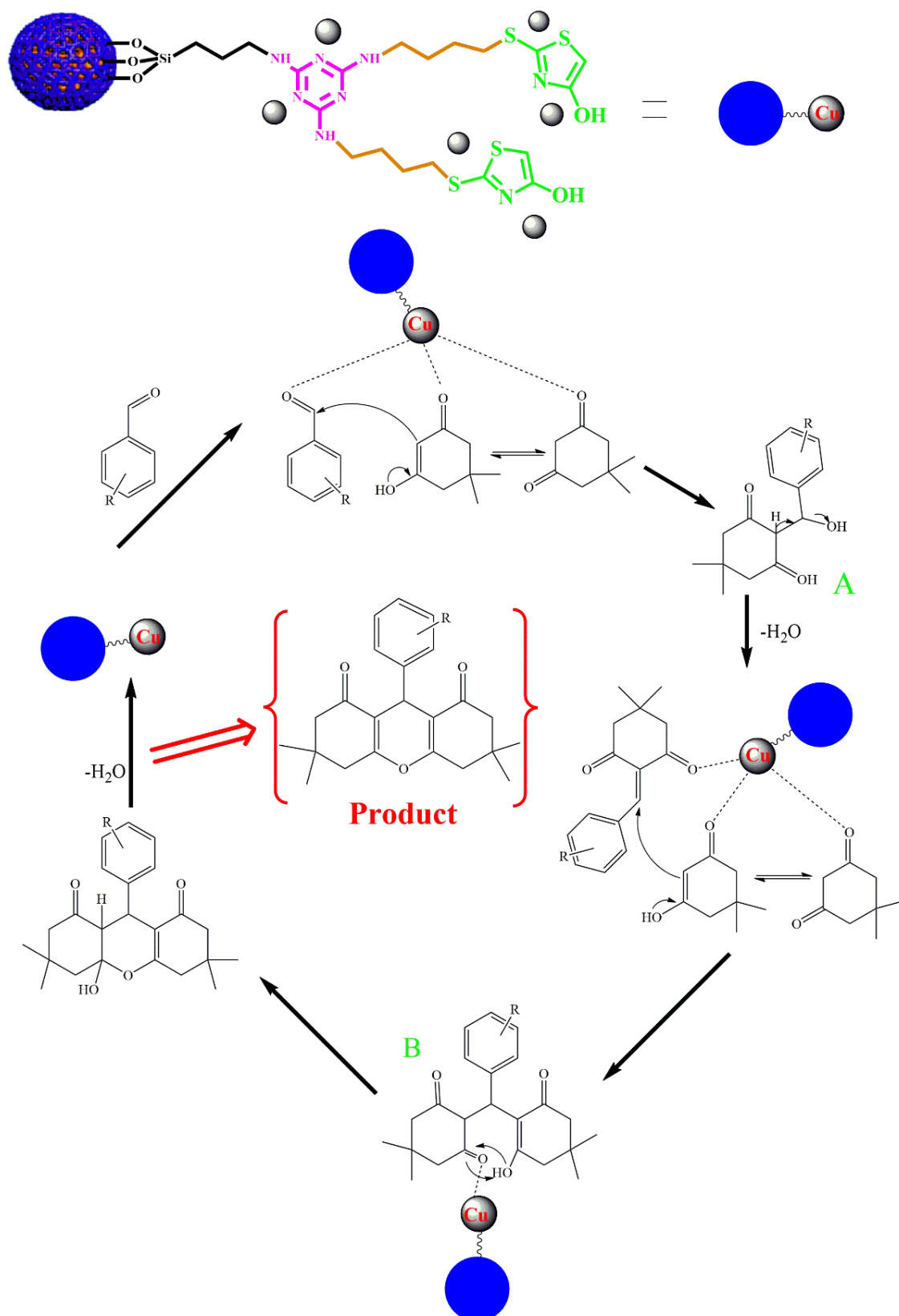
Scheme 3: Synthesis mechanism of xanthene derivatives by Fe_3O_4@SiO_2@Mel-Rh-Cu
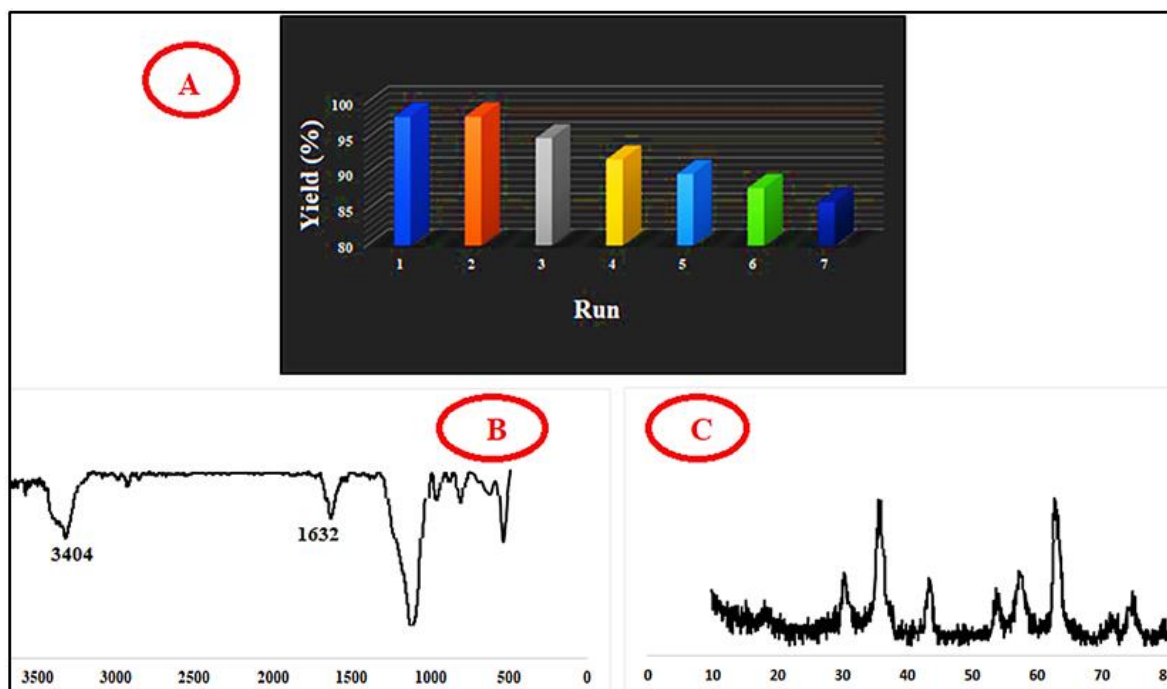
**Figure 9:** (A) Catalyst reusability diagram of the model reaction, (B) IR spectra of Fe$_3$O$_4$@SiO$_2$@Mel-Rh-Cu reused after seven cycles, and (C) XRD patterns of Fe$_3$O$_4$@SiO$_2$@Mel-Rh-Cu reused after eleven cycles

Instrumentation

Separation, detection and quantification of the extracted analyte was performed using a Waters HPLC instrument equipped with a dual UV-Vis detector model 2487 (Waters Assoc, Milford, MA, USA), a binary solvent pump model 1525 and an injection valve (Rheodyne 7725i (Cotati, CA, USA)) containing a 20-µL sample loop. Separation of the selected analytes was performed at room temperature on a Waters Symmetry ® reversed phase C18 column (25 mm × 4.6 mm I.D., 5 µm particle size). The analyte was eluted by an isocratic program at the flow rate of 1.0 mL min^{-1}. The mobile phase consisted of acetonitrile and water (80:20). The UV detector was set at 239 nm. Diazinon, was eluted at 6.1 min.

MSPE Procedure

To investigate the performance of the MSPE method (Magnetic solid-phase extraction) based on the prepared sorbent for diazinon extraction, the working solution of diazinon (100 µL^{-1}) was prepared and used. The initial step was screening using one factor at a time methodology and the second was optimization by Box-Behnken experimental design (BBD) to investigate optimal extraction conditions. Therefore, after examining the factors affecting the extraction process, the best condition of extraction was achieved. The exact values of each of the parameters depend on the values determined by the BBD table, but in general, the procedure was as follows:

10 ml of the sample containing the target analyte was introduced into the extraction tube (pH=7). A precise amount of adsorbent (7 mg) was subsequently added to the tube and thoroughly mixed by sonication for 15 min. The mixture was then subjected to an external magnet. The supernatant was decanted. At this juncture, an appropriate volume of desorption solvent (25 µL of methanol), as per the BBD table, was added to the precipitated adsorbents and sonicated for 1 min. For chemical analysis, 20 µL of the resultant mixture was injected into the HPLC-UV.

Design of Experiments and Optimizing (DOE)

In the next step, the mathematical modeling and assessment of responses were conducted using the Minitab software. RSM optimization

(Response surface methodology) is a key application of DOE. Various design techniques have been introduced in this method, and in this study, due to the extensive number of tests required and the potential interactions between the parameters, the BBD (Box-Behnken Design) was employed to identify the interferences among them and determine the optimal levels of these variables.

BBD enables the estimation of model parameters and necessitates fewer trials in the case of three variables. As such, five quantitative variables, namely the amount of sorbent, extraction time, ionic strength, desorption time, and eluent volume were estimated, and 46 runs were randomly designed based on them. Three-dimensional surface plots or contour plots were used to graphically display the relationship and interaction between the dependent variables and the absorption as the response.

Method Evaluation

To estimate the validity of the proposed technique, the performance metrics, the limit of detection (LOD), the linear dynamic range (LDR), the limit of quantification (LOQ), the enrichment factor (EF), and the relative standard deviations (RSD), were calculated. The target analyte concentration range is called LDR, where the amount of signal is proportional to the analyte concentration. A series of 9 extraction experiments were done with 9 different concentrations of 0.5, 1, 2, 5, 10, 20, 50, 100, and 200 µg L^{-1} of the chosen analyte in DI water. The linear range of diazinon was obtained in 0.5-200 µg L^{-1}. The coefficients of determination (R^2) for diazinon were 0.9985. The LODs and LOQs were determined based on the S/N=3 and 10, respectively. The limit of detection (LOD) of the technique for diazinon was 0.08 µg L^{-1}. Relative standard deviation (RSD %) values for having 10 µg L^{-1}, 50 µg L^{-1}, and 100 µg L^{-1} were also obtained between 5.3% and 6.2%. The following equation (EF: The enrichment factor) is used to calculate the concentration of the extracted analyte in the optimal eluent and the primary

concentration of the target analyte (Equation (1)):

$$EF = \frac{C_e}{C_0} \tag{1}$$

Where,

C_0 : the initial concentration in the sample solution

Ce: the final concentration of the analytes in the eluent

The estimated EF was 69. The mechanism for the extraction of the target analyte from the sample solution to the sorbent might be owing to the π-π stacking interaction, hydrogen bonding, and Van der Waals interaction between selected pesticides and the synthesized sorbent.

Real Sample Analysis

To evaluate the accuracy and capability of the technique, real sample analysis was used. For the quantitative determination of analytes, the addition technique was used as a standard. In order to accomplish this, three different concentrations (2, 5, and 10 µg/liter) were added to the samples and each concentration was replicated three times (n = 3). Also, relative recovery and spike recovery were calculated. Relative recovery (RR) was defined as the ratio of the distinguished analyte in real samples and pure water samples spiked with the same amount of analyte were measured for concentration. Spiking recovery was calculated using the following equation:

$$Spiking\ Recovery = \frac{C_{found} - C_{real}}{C_{added}} \tag{2}$$

Where,
C$_{found}$: the concentration after MSPE
C$_{real}$: the spiked concentration into the real sample
C$_{added}$: the concentrations of the analyte (µg L-1) in the real sample

Also, by repeating the test three times, the value of RSD% was obtained (Table 4). According to the obtained data, it can be confirmed that the above technique is suitable for the desired analyte in real samples.

Table 4: The results of the analysis of selected analytes in real samples

		Diazinon		
Orange	**Measured**	5.3		
	Added	2.00	5.00	10.00
	Found	7.4	10.2	15.20
	SR[a] (%)	105.00	98.00	99.00
	RR[b] (%)	98.00	95.00	93.00
	RSD% n=3	3.9		
Agricultural wastewater	**Measured**	3.2		
	Added	2.00	5.00	10.00
	Found	5.3	7.90	12.80
	SR (%)	105.00	94 .00	96.00
	RR (%)	102.00	98.00	97.00
	RSD% n=3	2.60		

[a] *Spiking recovery percentage*
[b] *Relative recovery percentage*

Conclusion

In this study, we have fabricated a new catalyst from rhodanine (whose derivatives have medicinal properties), melamine linker (which is utilized in the polymer industry), and then immobilized inexpensive copper metal ions on it. The $Fe_3O_4@SiO_2@Mel$-Rh-Cu was distinguished by some techniques like FT-IR, TGA, XRD, VSM, FE-SEM, EDX, and ICP. The prepared $Fe_3O_4@SiO_2@Mel$-Rh-Cu can be exploited as a remarkable, novel, and reusable catalyst for Xanthene synthesis. Among the advantages of the synthesized catalyst, we can mention the green conditions (without solvents) of the reaction, the high efficiency of the products in a short period, and suitable temperature conditions. Furthermore, it can be easily collected from the reaction environment and reused up to seven times.

The prepared sorbent was also used for the MSPE of diazinon followed by quantification through HPLC-UV. The proposed technique has the capability of separation and preconcentration in one step. Here, the extraction efficiency of the technique was improved by designing an optimization experiment of important and influencing variables, and then the figure of merit of the method was calculated. Furthermore, no matrix effect was observed with this technique. In summary, the results presented in the manuscript show that the proposed technique is satisfactory for the designation of small amounts quantities amounts of toxins in real samples.

Acknowledgments

ORCID

Sahar Peiman
https://orcid.org/0009-0000-7509-9277
Behrooz Maleki
https://orcid.org/0000-0002-0322-6991
Milad Ghani
https://orcid.org/0000-0003-1210-1856

References

[1]. Al-Jumaili M.H.A., Hamad A.A., Hashem H.E., Hussein A.D., Muhaidi M.J., Ahmed M.A., Albanaa, A.H.A., Siddique F., Bakr E.A., Comprehensive review on the Bis–heterocyclic compounds and

their anticancer efficacy, *Journal of Molecular Structure*, 2023, **1271**:133970 [Crossref], [Google Scholar], [Publisher]

[2]. Baharfar R., Peiman S., Maleki B., Fe$_3$O$_4$@ SiO$_2$@D-NHCS-Tr as an efficient and reusable catalyst for the synthesis of indol-3-yl-4 H-chromene via a multi-component reaction under solvent-free conditions, *Journal of Heterocyclic Chemistry*, 2021, **58**:1302 [Crossref], [Google Scholar], [Publisher]

[3]. Baghernejad B., Zakariayi A., One-Pot synthesis of oxindoles derivatives as effective antimicrobial agents by nano-magnesium aluminate as an effective aatalyst, *Asian Journal of Nanoscience and Materials*, 2022, **5**:225 [Crossref], [Publisher]

[4]. Baranwal J., Kushwaha S., Singh S., Jyoti A., A review on the synthesis and pharmacological activity of heterocyclic compounds, *Current Physical Chemistry*, 2023, **13**:2 [Crossref], [Google Scholar], [Publisher]

[5]. Swami M.B., Nagargoje G.R., Mathapati S.R., Bondge A.S., Jadhav A.H., Panchgalle S.P., More V., A Magnetically Recoverable and Highly Effectual Fe$_3$O$_4$ Encapsulated MWCNTs Nano-Composite for Synthesis of 1,8-Dioxo-octahydroxanthene Derivatives. *Journal of Applied Organometallic Chemistry*, 2023, **3**:184 [Crossref], [Publisher]

[6]. Allahresani A., Ghorbanian F., Nasseri M.A., Kazemnejadi M., Isolation and Characterization of Bis(2-ethylheptyl) phthalate from Cynodon dactylon (L.) and Studies on Catalytic Activity of Its Cu (II) Complex in the Green Preparation of 1,8-Dioxo-octahydroxanthenes. *Journal of Applied Organometallic Chemistry*, 2022, **2**:39 [Crossref], [Publisher]

[7]. Naderi S., Sandaroos R., Peiman S., Maleki B., Novel crowned cobalt (II) complex containing an ionic liquid: A green and efficient catalyst for the one-pot synthesis of chromene and xanthene derivatives starting from benzylic alcohols, *Journal of Physics and Chemistry of Solids*, 2023, **180**:111459 [Crossref], [Google Scholar], [Publisher]

[8]. Baghernejad B., Alikhani M., Nano-cerium oxide/aluminum oxide as an efficient catalyst for the synthesis of xanthene derivatives as potential antiviral and anti-inflammatory agents, *Journal of*

Applied Organometallic Chemistry, 2022, **2**:140 [Crossref], [Publisher]

[9]. Zare A., Mostaghar F., Construction of a Novel Magnetic Nanomaterial, and its Utility as an Effectual Catalyst for the Fabrication of 1, 8-Dioxo-Octahydroxanthenes, *Chemical Methodologies*, 2023, **8**:23 [Crossref], [Publisher]

[10]. Baharfar R., Peiman S., Mohseni M., Synthesis and Antibacterial Activity of a Novel Class of Benzylidenrhodanine Based Furan Derivatives, *Letters in Organic Chemistry*, 2014, **11**:393 [Google Scholar], [Publisher]

[11]. Tomasic T., Masic L.P., Rhodanine as a privileged scaffold in drug discovery, *Current Medicinal Chemistry*, 2009, **16**:1596 [Crossref], [Google Scholar], [Publisher]

[12]. Kaminskyy D., Kryshchyshyn A., Lesyk R., Recent developments with rhodanine as a scaffold for drug discovery, *Expert Opinion on Drug Discovery*, 2017, **12**:1233 [Crossref], [Google Scholar], [Publisher]

[13]. Baharfar R., Asghari S., Peiman S., Synthesis of novel rhodanine based functionalized furans from the reaction of tert-butyl isocyanide with acetylenic esters in the presence of rhodanine acetic acid derivatives, *Arabian Journal of Chemistry*, 2019, **12**:1496 [Crossref], [Google Scholar], [Publisher]

[14]. Alinezhad H., Amiri P.H.T., Tavakkoli S.M., Muhiebes R.M., Mustafa Y.F., Progressive Types of Fe$_3$O$_4$ Nanoparticles and Their Hybrids as Catalysts, *Journal of Chemical Reviews*, 2022, **4**:288 [Crossref], [Google Scholar], [Publisher]

[15]. Rabiei M., zeynizadeh B., Khanmirzaee M., The immobilized SbFx species on copper or nickel ferrite as magnetic nanocatalysts for fast and convenient reduction and reductive acetylation of nitroarenes as well Acetylation farylamines, *Journal of Applied Organometallic Chemistry*, 2021, **1**:174 [Crossref], [Google Scholar], [Publisher]

[16]. Khan M., Khan S., Omar M., Sohail M., Ullah I., Nickel and Cobalt Magnetic Nanoparticles (MNPs): Synthesis, Characterization, and Applications, *Journal of Chemical Reviews*, 2024, **6**:94 [Crossref], [Publisher]

[17]. Mousavi Ghahfarokhi S.E., Helfi K., Zargar Shoushtari M., Synthesis of the Single-Phase

Bismuth Ferrite ($BiFeO_3$) Nanoparticle and Investigation of Their Structural, Magnetic, Optical and Photocatalytic Properties, *Advanced Journal of Chemistry, Section A*, 2022, **5**:45 [Crossref], [Google Scholar], [Publisher]

[18]. Hakimi F., Taghvaee M., Golrasan E., Synthesis of Benzoxazole Derivatives Using Fe_3O_4@SiO_2-SO_3H Nanoparticles as a Useful and Reusable Heterogeneous Catalyst Without Using a Solvent, *Advanced Journal of Chemistry, Section A*, 2023, **6**:188 [Crossref], [Google Scholar], [Publisher]

[19]. Ghasemi S., Badri F., Rahbar Kafshboran H., Pd Catalyst Supported Thermo-Responsive Modified Poly(N-isopropylacrylamide) Grafted Fe_3O_4@CQD@Si in Heck Coupling Reaction, *Asian Journal of Green Chemistry*, 2024, **8**:39 [Crossref], [Google Scholar], [Publisher]

[20]. Peiman S., Baharfar R., Maleki B., Immobilization of trypsin onto polyamidoamine dendrimer functionalized iron oxide nanoparticles and its catalytic behavior towards spirooxindole-pyran derivatives in aqueous media, *Materials Today Communications*, 2021, **26**:101759 [Crossref], [Google Scholar], [Publisher]

[21]. Peiman S., Baharfar R., Hosseinzadeh R., CuI NPs immobilized on a ternary hybrid system of magnetic nanosilica, PAMAM dendrimer and trypsin, as an efficient catalyst for A3-coupling reaction, *Research on Chemical Intermediates*, 2022, **48**:1365 [Crossref], [Google Scholar], [Publisher]

[22]. Abd El-Aal M., Said A.E.-A.A., Goda M.N., Zeid E.F.A., Ibrahim S.M., Fe_3O_4@CMC-Cu magnetic nanocomposite as an efficient catalyst for reduction of toxic pollutants in water, *Journal of Molecular Liquids*, 2023, **385**:122317 [Crossref], [Google Scholar], [Publisher]

[23]. Boroumand H., Alinezhad H., Maleki B., Peiman S., Triethylenetetramine-grafted magnetic graphene oxide (Fe_3O_4@GO-NH_2) as a reusable heterogeneous catalyst for the one-pot synthesis of 2-amino-4 H-benzopyran derivatives, *Polycyclic Aromatic Compounds*, 2023, **43**:7853 [Crossref], [Google Scholar], [Publisher]

[24]. Naderi S., Sandaroos R., Peiman S., Maleki B., Novel crowned cobalt (II) complex containing an ionic liquid: A green and efficient catalyst for the one-pot synthesis of chromene and xanthene derivatives starting from benzylic alcohols, *Journal of Physics and Chemistry of Solids*, 2023, **180**:111459 [Crossref], [Google Scholar], [Publisher]

[25]. Maleki B., Sandaroos R., Naderi S., Peiman S., A crowned manganese-based Schiff complex supported on nanocellulose as an efficient and sustainable heterogeneous catalyst for the oxidation of benzyl alcohols, *Journal of Organometallic Chemistry*, 2023, **990**:122666 [Crossref], [Google Scholar], [Publisher]

[26]. Maleki B., Sandaroos R., Peiman S., Mn (III) Schiff base complexes containing crown ether rings immobilized onto MCM-41 matrix as heterogeneous catalysts for oxidation of alkenes, *Heliyon*, 2023, **9**:e15041 [Crossref], [Google Scholar], [Publisher]

[27]. Sandaroos R., Maleki B., Naderi S., Peiman S., Efficient synthesis of sulfones and sulfoxides from sulfides by cobalt-based Schiff complex supported on nanocellulose as catalyst and Oxone as the terminal oxidant, *Inorganic Chemistry Communications*, 2023, **148**:110294 [Crossref], [Google Scholar], [Publisher]

[28]. Maleki B., Jafari-Soghieh F., Alinezhad H., Ghani M., jamshidi A., Development of PAMAM dendrimer-modified magnetic polyoxometalate: A novel platform to reinforce mechanical and thermal properties of diglycidyl ether of bisphenol A/isophorone diamine hardener epoxy, *High Performance Polymers*, 2022, **34**:768 [Crossref], [Google Scholar], [Publisher]

[29]. Darvishy S., Alinezhad H., Vafaeezadeh M., Peiman S., Maleki B., S-(+) Camphorsulfonic acid glycine (csag) as surfactant-likes brønsted acidic ionic liquid for one-pot synthesis of ß-amino carbonyl, *Polycyclic Aromatic Compounds*, 2022, 1 [Crossref], [Google Scholar], [Publisher]

[30]. Gholamian F., Hajjami M., Sanati A.M., Ni-Rhodanine complex supported on FSM-16 as mesoporous silica support: Synthesis, characterization and application in synthesis of tri and tetrasubstituted imidazoles and 3, 4-

dihydropyrimidine-2-(1*H*)-Ones, *Silicon*, 2020, **12**:2121 [Crossref], [Google Scholar], [Publisher]

[31]. Valiey E., Dekamin M.G., Alirezvani Z., Melamine-modified chitosan materials: An efficient and recyclable bifunctional organocatalyst for green synthesis of densely functionalized bioactive dihydropyrano [2, 3-c] pyrazole and benzylpyrazolyl coumarin derivatives, *International Journal of Biological Macromolecules*, 2019, **129**:407 [Crossref], [Google Scholar], [Publisher]

[32]. Bhale P.S., Dongare S.B., Mule Y.B., An efficient synthesis of 1, 8-dioxooctahydroxanthenes catalysed by thiourea dioxide (TUD) in aqueous media, *Chemical Science Transactions*, 2015, **4**:246 [Crossref], [Google Scholar], [PDF]

[33]. Gong K., Fang D., Wang H.L., Zhou X.L., Liu Z.L., The one-pot synthesis of 14-alkyl-or aryl-14H-dibenzo [a, j] xanthenes catalyzed by task-specific ionic liquid, *Dyes and Pigments*, 2009, **80**:30 [Crossref], [Google Scholar], [Publisher]

[34]. Rekunge D.S., Khatri C.K., Chaturbhuj G.U., Rapid and efficient protocol for Willgerodt–Kindler's thioacetamides catalyzed by sulfated polyborate, *Monatshefte für Chemie-Chemical Monthly*, 2017, **148**:2091 [Crossref], [Google Scholar], [Publisher]

[35]. Mohammadi R., Eidi E., Ghavami M., Kassaee M.Z., Chitosan synergistically enhanced by successive Fe$_3$O$_4$ and silver nanoparticles as a novel green catalyst in one-pot, three-component synthesis of tetrahydrobenzo [α] xanthene-11-ones, *Journal of Molecular Catalysis A: Chemical*, 2014, **393**:309 [Crossref], [Google Scholar], [Publisher]

[36]. Ghassamipour S., Ghashghaei R., Zirconium dodecylphosphonate promoted synthesis of xanthene derivatives by condensation reaction of aldehydes and β-naphthol or dimedone in green media, *Monatshefte für Chemie-Chemical Monthly*, 2015, **146**:159 [Crossref], [Google Scholar], [Publisher]

[37]. Niknam K., Panahi F., Saberi D., Mohagheghnejad M., Silica-bonded S-sulfonic acid as recyclable catalyst for the synthesis of 1, 8-dioxo-decahydroacridines and 1, 8-dioxo-octahydroxanthenes, *Journal of Heterocyclic Chemistry*, 2010, **47**:292 [Crossref], [Google Scholar], [Publisher]

[38]. Maghsoodlou M.T., Habibi-Khorassani S.M., Shahkarami Z., Maleki N., Rostamizadeh M., An efficient synthesis of 2, 2′-arylmethylene bis (3-hydroxy-5, 5-dimethyl-2-cyclohexene-1-one) and 1, 8-dioxooctahydroxanthenes using ZnO and ZnO–acetyl chloride, *Chinese Chemical Letters*, 2010, **21**:686 [Crossref], [Google Scholar], [Publisher]

[39]. Rezayati S., Hajinasiri R., Erfani Z., Rezayati S., Afshari-sharifabad S., Boric acid as a highly efficient and reusable catalyst for the one-pot synthesis of 1, 8-dioxo-octahydroxanthenes under solvent-free conditions, *Iranian Journal of Catalysis*, 2014, **4**:157 [Google Scholar]

[40]. Moradi L., Mirzaei M., Immobilization of Lewis acidic ionic liquid on perlite nanoparticle surfaces as a highly efficient solid acid catalyst for the solvent-free synthesis of xanthene derivatives, *RSC Advances*, 2019, **9**:19940 [Crossref], [Google Scholar], [Publisher]

[41]. Song G., Wang B., Luo H., Yang L., Fe3+-montmorillonite as a cost-effective and recyclable solid acidic catalyst for the synthesis of xanthenediones, *Catalysis Communications*, 2007, **8**:673 [Crossref], [Google Scholar], [Publisher]

[42]. Hekmatshoar R., Majedi S., Bakhtiari K., Sodium selenate catalyzed simple and efficient synthesis of tetrahydro benzo [b] pyran derivatives, *Catalysis Communications*, 2008, **9**:307 [Crossref], [Google Scholar], [Publisher]

[43]. Khurana J.M., Magoo D., pTSA-catalyzed one-pot synthesis of 12-aryl-8, 9, 10, 12-tetrahydrobenzo [a] xanthen-11-ones in ionic liquid and neat conditions, *Tetrahedron Letters*, 2009, **50**:4777 [Crossref], [Google Scholar], [Publisher]

[44]. Wang H.J., Ren X.Q., Zhang Y.Y., Zhang Z.H., Synthesis 12-aryl or 12-alkyl-8, 9, 10, 12-tetrahydrobenzo [a] xanthen-11-one derivatives catalyzed by dodecatungstophosphoric acid, *Journal of the Brazilian Chemical Society*, 2009, **20**:1939 [Crossref], [Google Scholar], [Publisher]

[45]. Khurana J.M., Magoo D., pTSA-catalyzed one-pot synthesis of 12-aryl-8, 9, 10, 12-tetrahydrobenzo [a] xanthen-11-ones in ionic liquid and neat conditions, *Tetrahedron Letters*,

2009, **50**:4777 [Crossref], [Google Scholar], [Publisher]

[46]. Shitole N.V., Sapkal S., Shingate B.B., Shingare M.S., A simple and green synthesis of tetrahydrobenzo [α]-xanthen-11-one using peg-400 as efficient and recyclable reaction media, *Bulletin of the Korean Chemical Society*, 2011, **32**:35 [Crossref], [Google Scholar], [PDF]

Use your device to scan and read the article online